Open Access

Recent Progress in Materials

LIDSEN Publishing Inc.

Original Research

Construction and Evaluation of a Modular Anthropomorphic Phantom of the Skull with an Exchangeable Specimen Jar to Optimize the Radiological Examination of Temporal Bone Pathology

Malin Vestin Fredriksson [1], Love Kull [2], Anton Rönnblom [1], Lennart Flygare [3], Diana Berggren [4], Krister Tano [1, *]

1. Department of Clinical Sciences, Otorhinolaryngology, Sunderby Research Unit, Umeå University, Umeå, Sweden; E-Mails: malin.vestin-fredriksson@norrbotten.se; anton.ronnblom@norrbotten.se; krister.tano@umu.se
2. Department of Medical Physics, Sunderby Hospital, Luleå, Sweden; E-Mail: love.kull@norrbotten.se
3. Department of Radiation Sciences, Umeå University, Umeå, Sweden; E-Mail: lennart.flygare@umu.se
4. Department of Clinical Sciences, Otorhinolaryngology, Umeå University, Umeå, Sweden; E-Mail: diana.berggren@umu.se

* **Correspondence:** Krister Tano; E-Mail: krister.tano@umu.se

Academic Editor: Ziyad S. Haidar

Special Issue: Advances, Trends and Prospects for Materials in the Head and Neck

Recent Progress in Materials
2024, volume 6, issue 3
doi:10.21926/rpm.2403018

Received: March 26, 2024
Accepted: July 07, 2024
Published: July 25, 2024

Abstract

To develop a modular anthropomorphic phantom to evaluate the performance of radiological techniques for detecting pathologies in the temporal bone region. A phantom was constructed using a human skull, temporal bone specimen, and 3D-printed contour of a human skull. The human skull was embedded in tissue-equivalent plastic, with a cavity to hold the plastic jars containing the exchangeable freshly frozen human temporal bones. Subsequently, stepwise introduction and examination of different clinicopathological scenarios were conducted. Radiological images were nearly identical to those acquired from

patients using computed tomography (CT) and cone beam computed tomography (CBCT). The radiological attenuation of polyurethane plastic (PUR) and alginate were similar to those of the soft tissues of living human patients. The mean Hounsfield unit values of the CT slices representing tissue at the brain and temporal bone level were 184 and 171 in the phantom and patient groups, respectively. The modular phantom developed in this study can evaluate radiological techniques and diagnostic possibilities without exposing patients to radiation. To our knowledge, no such modular phantom has been reported in the literature or made available commercially.

Keywords
Anthropomorphic phantoms; radiological techniques; temporal bones; computed tomography; cone beam computed tomography

1. Introduction

Phantoms are essential tools for evaluating the performance of radiological systems. Two main types of phantoms are available commercially: anthropomorphic and calibration phantoms. Anthropomorphic phantoms simulate the human body and can be used for various applications, such as optimizing parameters and image reconstruction techniques. Calibration phantoms, explicitly designed for quality control, quality assurance, and system acceptance testing, use a more straightforward design, such as a cylinder or plate, to assess image quality parameters.

Clinical trials [1, 2] remain the gold standard for optimizing and evaluating medical imaging systems. Anthropomorphic phantoms offer several benefits in assessing the potential risks and benefits of radiological examinations without exposing patients to radiation [3, 4]. These phantoms have enabled the optimization of examinations and comparison of the impact of different parameters on the same participant, as well as the simulation of known pathologies to compare diagnostic accuracy. However, prefabricated anthropomorphic phantoms designed for examining the skull, such as Alderson phantoms [5], are not adjustable, which limits the evaluation of various pathologies.

Radiological assessment is crucial in ensuring surgical success and risk minimization in otological surgery. Thus, it is important to obtain accurate preoperative information [6]. Dedicated models capable of performing clinical tasks have not been developed for image quality studies [7]. Therefore, this study aimed to develop a modular anthropomorphic phantom to allow the insertion of natural temporal bone specimens that can be changed easily. Given the complex anatomy and sensitive structures involved in temporal bone surgery, the phantom enables the evaluation of normal and pathological temporal bone anatomy. This could facilitate the comparison of different radiological modalities, such as computed tomography (CT), cone-beam computed tomography (CBCT) [8, 9], and photon-counting CT (PCCT) [10].

2. Methods and Materials

A modular anthropomorphic phantom with a specially designed chamber for the fixation of exchangeable temporal bones was developed in this study.

2.1 Polyurethane Plastic as a Soft Tissue Equivalent

The materials used for the construction of anthropomorphic phantoms should possess radiological attenuation properties similar to those of human tissues in the same region. This study subjected different materials and polyurethane (PUR) plastic (Ebalta Kunststoff GmbH, SG 130/PUR 11) to radiological evaluations. The radiological attenuation of PUR plastic was compared with those of other suitable materials, such as PMMA (Plexiglas®) and beef. PMMA was used in this study as it is often used as an equivalent to water in radiological phantoms [11], whereas beef was used owing to its similarity to soft tissue.

A PMMA/Plexiglas computed tomography dose index (CTDI) phantom (16 cm in diameter) was used to create two molds. PUR was then cast in one mold, whereas minced beef was packed in the other mold and frozen.

The radiological attenuation of the three different materials was compared by scanning each phantom using a Canon Aquilion ONE (Canon Medical Systems Corporation Ötawara, Tochigi, Japan) multi-slice CT scanner. The Hounsfield unit (HU) value [12] for a homogeneous region on the acquired image was evaluated for each material using an area of interest (ROI) in the CT system software.

PUR was used to simulate all soft tissues present in a human's head and neck region owing to its similarities with soft tissue.

This study used three-dimensional (3D) models representing a human skull, temporal bone specimen, and the skin covering a human head to construct the phantom. Computer-aided design (CAD) was used to build the 3D parts to complement the skull and head models (Figure 1).

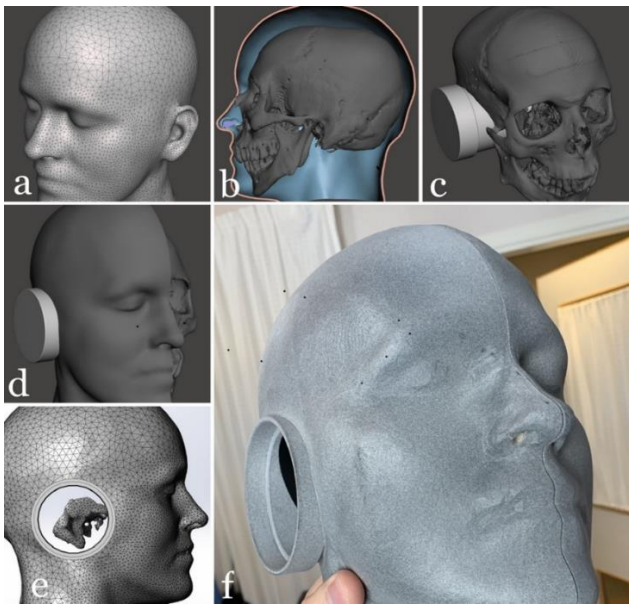

Figure 1 a) A hollow three-dimensional (3D) model of the human head obtained from CT data imported into Meshmixer via Horos that represents the outer shell of the human head. b) A 3D model of the dry skull imported into Meshmixer and positioned inside the model of the outer shell. c & d) A 3D model of the specimen jar imported into Meshmixer and positioned without and with the model of the outer shell. e) Export of the model(s) from Meshmixer to Solidworks to model the specimen jar holder. f) The 3D-printed shell of the anthropomorphic skull phantom.

Thin axial CT images were used to obtain the anatomical image data from the 3D models of the skull, temporal bone specimen, and human head. The image data were imported into Horos software [13] for segmentation (selecting tissues to export) and exported to a 3D file.

MeshMixer [14] was used for scaling and remodeling the 3D models. In addition, MeshMixer was also used to merge the 3D models and create the final hollow model of the head, representing the skin covering a human head.

SolidWorks [15] was used to design 3D models of objects, such as the specimen jar, for which the CT image data could not be obtained.

2.2 Creation of the Anthropomorphic Phantom

CT images of a human skull and temporal bone specimen were acquired to plan the merging of the skull and nylon shell, as explained below.

A 2-mm thick shell representing the skin covering the head resized to fit the skull was created to simplify the construction of the phantom. An existing CT image acquired by the first author was segmented and printed in an MJF 3D printer (Jet Fusion 3D 4210, HP Inc., Palo Alto, CA, USA) using nylon (PA12). CT examination revealed that the radiological attenuation of nylon plastic produced HU values similar to those of the skin covering the human head.

The human skull was then fixed in the nylon printed half without an access hole for the specimen jar. The second half was temporarily placed as a surgical guide for removing the temporal bone and adjacent structures, representing the volume of the specimen jar (Figure 2a & Figure 2b).

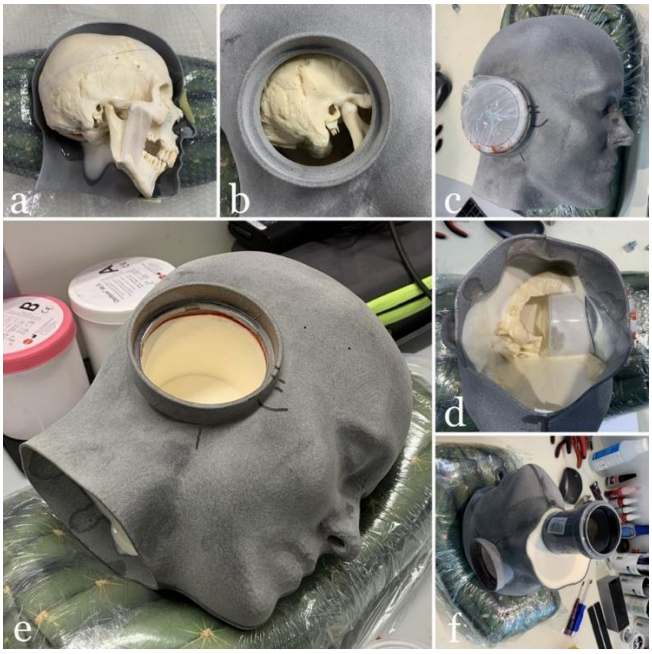

Figure 2 a) Dry skull positioned into one half of the shell and fixed with a small amount of PUR plastic. b) The second half of the shell is positioned and fixed temporarily to accommodate bone removal. c) Specimen jar in its position. d) Approximately half of the cavity is filled with PUR plastic. e) Most of the cavity was filled with PUR plastic while the specimen jar was removed. f) The last portion of the cavity filled with PUR plastic with a suitable mount (needed for an upright positioning during CBCT examinations) was inserted.

After removing the temporal bone, the two halves were glued together, and the specimen jar was positioned and treated with a release agent. PUR plastic was used to fill the cavity layer by layer as the curing process was highly exothermic. A mount was also incorporated into the neck of the phantom (Figures 2c-2f).

2.3 Adjustment and Fixation of the Temporal Bone Sample in the Phantom

The freshly frozen temporal bone was adjusted to fit into a plastic sample jar. This study aimed to align the temporal bone to an anatomically suitable position in the skull. The bone was positioned within the jar and surrounded by a removable alginate mass for stability. The alginate mass also replaced some of the absent human tissue and PUR plastic due to the phantom sample jar cavity. Ballistic gelatin has shown good soft tissue characteristics on radiological examinations [16] and has been used as an alternative to alginate. However, it was not used as it filled the air-filled spaces within the middle ear cavity owing to its viscosity despite various sealants. The orientation of the temporal bone was marked when it was fitted to the sample jar to ensure that the jar could be fitted in the correct anatomical position in the phantom. The correct position was confirmed via a CT examination and adjusted if necessary. A marking of the jar that corresponded to a marking of the phantom, “twelve o’clock,” was made to ensure reproducibility. The zygomatic arch and the borders of the mandible connecting to the access hole for the specimen jar were marked on the phantom. The visibility of the zygomatic arch and the external ear canal was maintained on the temporal bone specimen, and the position of “twelve o’clock” was marked (Figure 3a). The sample jar containing the temporal bone was stored in a freezer except when the tests were performed using CBCT/CT.

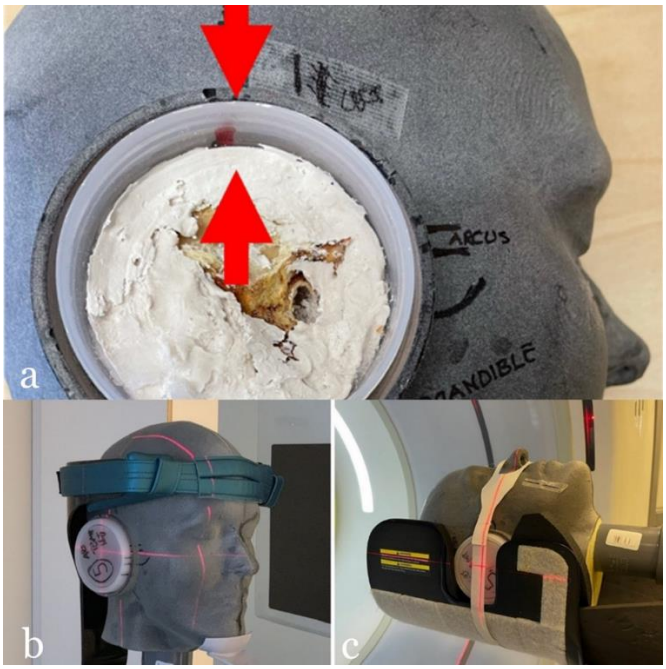

Figure 3 a) The temporal bone specimen in the sample jar aligned with the anatomic structures of the phantom. To achieve correct positioning, the arrow on the temporal bone should point to a corresponding line on the anthropomorphic skull phantom. b) The anthropomorphic skull phantom is positioned upright in the CBCT. c) The Phantom was positioned in a supine position for the CT examination.

2.4 Positioning of the Phantom during the Radiological Examinations

The phantom was positioned upright using a camera stand to the incorporated mount for the CBCT examination. A fixation headband was used in the same manner as when examining the patient. A scout (overview) was used to ensure the correct positioning of the phantom. The laser guidelines were adjusted, and marks were made on the phantom to ensure reproducibility (Figure 3b).

The phantom was positioned horizontally and supported by a standard headrest and foam cushions for the CT examination. The laser guidelines were adjusted, and corresponding marks were made on the phantom to ensure reproducibility (Figure 3c).

2.5 Optimization of the Examination Protocols for CBCT/CT

The parameters for each system were assessed per the flowchart below and found to improve the existing protocol (Figure 4). The parameters were selected based on subjective quality.

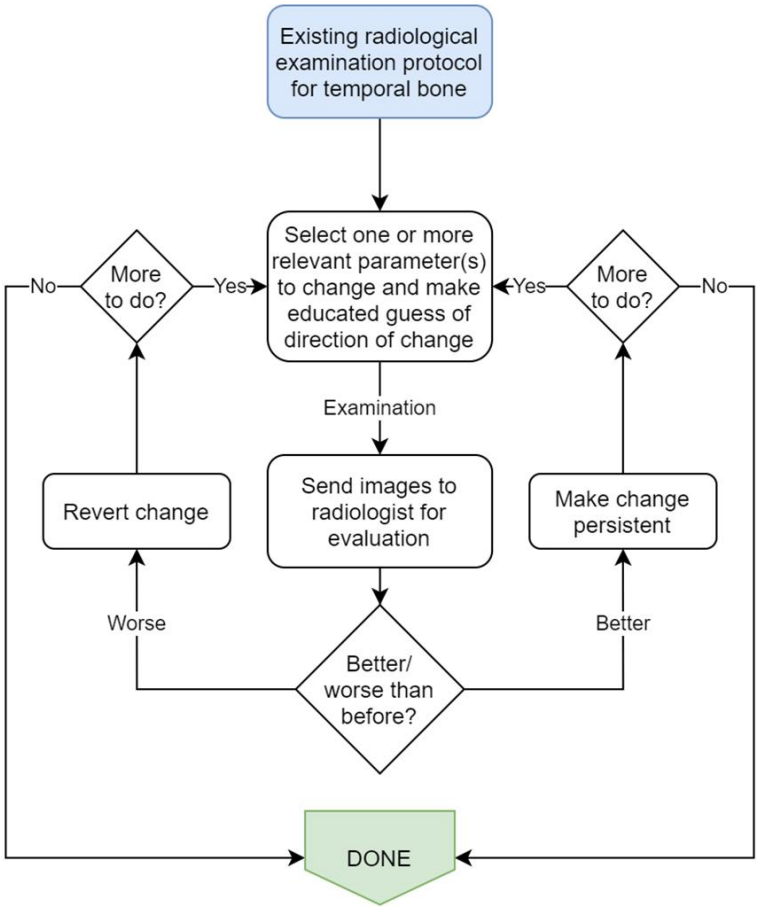

Figure 4 Optimization process flowchart.

Some parameters were split into multiple tracks and evaluated in parallel with other parameters. For instance, the tube voltage (kVp) was evaluated in two tracks for CT, 120 kVp and 140 kVp, and other parameters were varied within these tracks. The best track was selected when the tracks diverged significantly.

The radiation dose was, within reasonable limits, subordinate to image quality during optimization.

2.5.1 Cone Beam CT

System used:

- Morita 3D Accuitomo 170 (J Morita Corporation, Kyoto, Japan), a cone-beam CT scanner with a maximum volume of 120 × 170 mm, was used for head and neck examinations.

Evaluated:

- Exposure mode (standard, hi-fi, high-resolution mode)
- Rotation angle, 180° or 360° rotation
- Tube voltage (70, 80, and 90 kVp)
- Tube current (3, 5, 7, and 8 mA)
- Volume size (60 × 60, 80 × 80, 100 × 100, 140 × 100, and 140 × 50 mm^2)

Not evaluated, established protocol applied:

- Reconstruction slice thickness

2.5.2 Medical Multi-slice CT

Systems used:

- GE Optima CT660 (GE Healthcare, Waukesha, WI, USA) is a multi-slice medical CT scanner with a maximum beam width of 40 mm capable of whole-body axial and spiral acquisitions.
- GE Revolution CT (GE Healthcare, Waukesha, WI, USA) is a multi-slice medical CT scanner with a maximum beam width of 160 mm capable of whole-body axial and spiral acquisitions.

Evaluated two tracks in parallel (120 kVp and 140 kVp):

- Level of iterative reconstruction
- Reconstruction filter kernel
- System-specific reconstruction techniques
- Tube current (mA)
- Focal spot size (depending on the above)

Not evaluated, established practice applied:

- Rotation time, highest possible used (i.e., slowest rotation)
- Pitch factor, lowest factor possible (only applicable for GE Optima)
- Collimation, the thinnest possible used
- Reconstruction slice thickness, thinnest possible used

2.6 Phantom Evaluation

Ten frozen human temporal bones were placed in the phantom and evaluated using Optima CT or Revolution CT. The acquired images were compared with ten pre-existing radiological images of patients with suspected middle ear pathology that had also been acquired using Optima CT or Revolution CT. Three smaller ROIs were placed at the rear of the skull in a region with mixed brain tissue in the human patients and the region containing PUR plastic in the phantom images. The mean HU value [4] was recorded for each ROI. An additional ROI representing the outline of the head was used to calculate the average HU value for all structures present within the ROI. Smaller

ROIs were used to compare the attenuation of the PUR plastic with that of human brain tissue. Larger ROIs were used to compare the average attenuation of the phantom in the axial plane with that of a human patient, which depicted the accuracy of the radiological environment created in the phantom compared with that observed in a living human.

This study was approved by the regional ethics committee of Umeå University (DNR: 2014-352-31). IBM SPSS Statistics for Windows (Version 29.0. Armonk, IBM Corp. Released 2022., NY: IBM Corp.) was used for descriptive statistical analysis. A p-value of < 0.05 was considered statistically significant.

3. Results

3.1 Materials Used to Construct the Phantom

The evaluation of the tissue-equivalent materials revealed that the radiological attenuation of PUR plastic was similar to that of soft tissue (minced beef) at different beam qualities. Thus, it could be used as a substitute for soft tissue in anthropomorphic phantoms.

CT evaluation of the PUR plastic yielded the following results.

As shown in Table 1, the radiological attenuation of PUR plastic was similar to that of soft tissue (minced beef) and superior to that of the gold standard PMMA.

Table 1 Hounsfield unit values (i.e., attenuation) for the tested materials.

kVp	HU PMMA	HU PUR	HU Minced meat
80	97.8	-18.9	-7.0
120	123.7	10.6	-4.2
135	128.8	13.7	-6.3

The HU value of PUR plastic was comparable with that of the soft tissue in the head and neck when used as a substitute for soft tissues in the phantom. The use of alginate was preferred over the use of ballistic gel for the fixation of the temporal bones in the jar, owing to the lower risk of intrusion of gel into the middle ear of the temporal bone (Figure 5). Alginate exhibited an attenuation of approximately 200 HU.

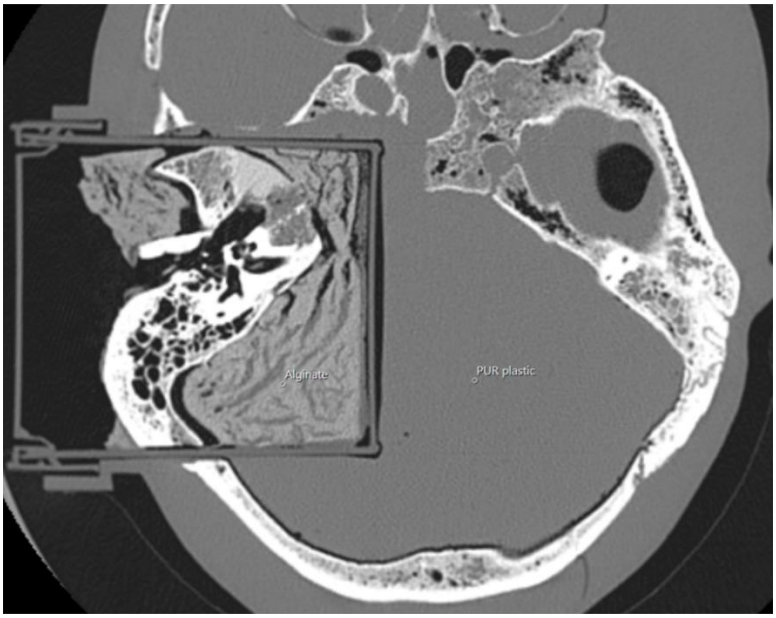

Figure 5 Axial image of the anthropomorphic phantom acquired at the height of the middle ear, with the specimen jar with human temporal bone in place.

The mean HU values of the brain in the phantom (Figure 6a) and the corresponding area in the human brain (Figure 6b) were 25 HU and 35 HU, respectively, indicating very good agreement. The mean value was calculated from 30 ROIs (10 temporal bones in the phantom and 10 consecutive patients).

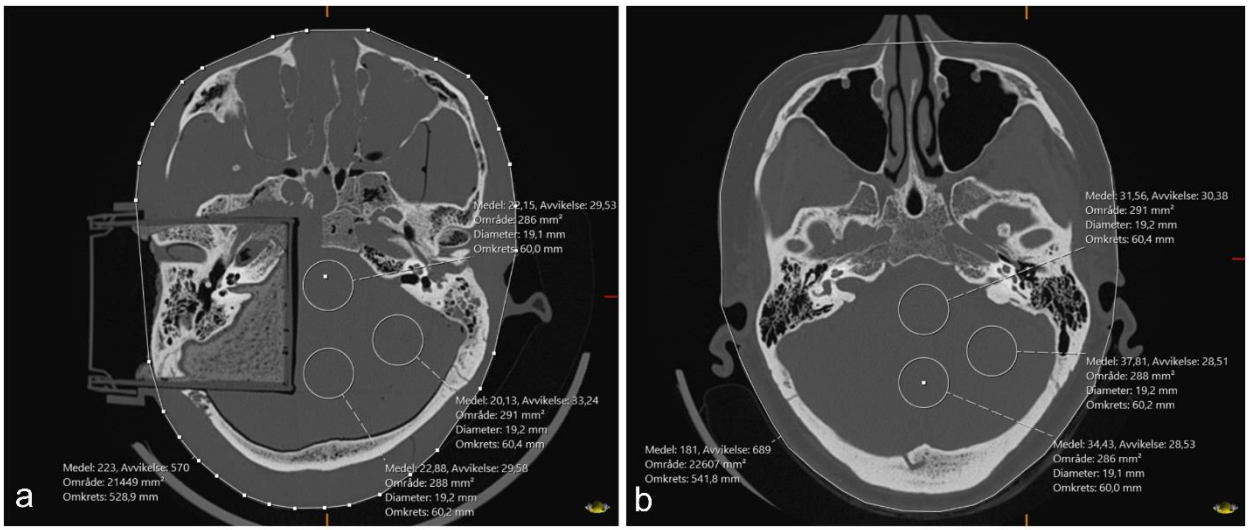

Figure 6 Comparison of the Hounsfield unit values, total mean of the slices, and mean for PUR and brain tissue. a) For the anthropomorphic skull phantom. b) For a representative human. Medel = Mean; Avvikelse = Standard deviation.

The mean HU value of the larger ROI containing the entire area of the phantom head with the ten temporal bones placed in the phantom (184 HU, with a mean standard deviation of 595 HU) was comparable with the mean HU of the corresponding region in the human skull (171 HU, with a mean standard deviation of 645 HU) in ten consecutive patients (Figure 6).

To determine the mean HU value in the small ROIs, a comparative analysis was performed between two groups with a phantom containing ten different temporal bones and another group of ten consecutive patients. The Mann-Whitney U test revealed a statistically significant difference ($p < 0.05$) between the HU values of the two groups (Figure 7a). However, the difference in the mean value was only 10 HU, a fraction of the standard deviation within the brain tissue. It did not indicate clinical or technical significance in the CT assessment of the temporal bone.

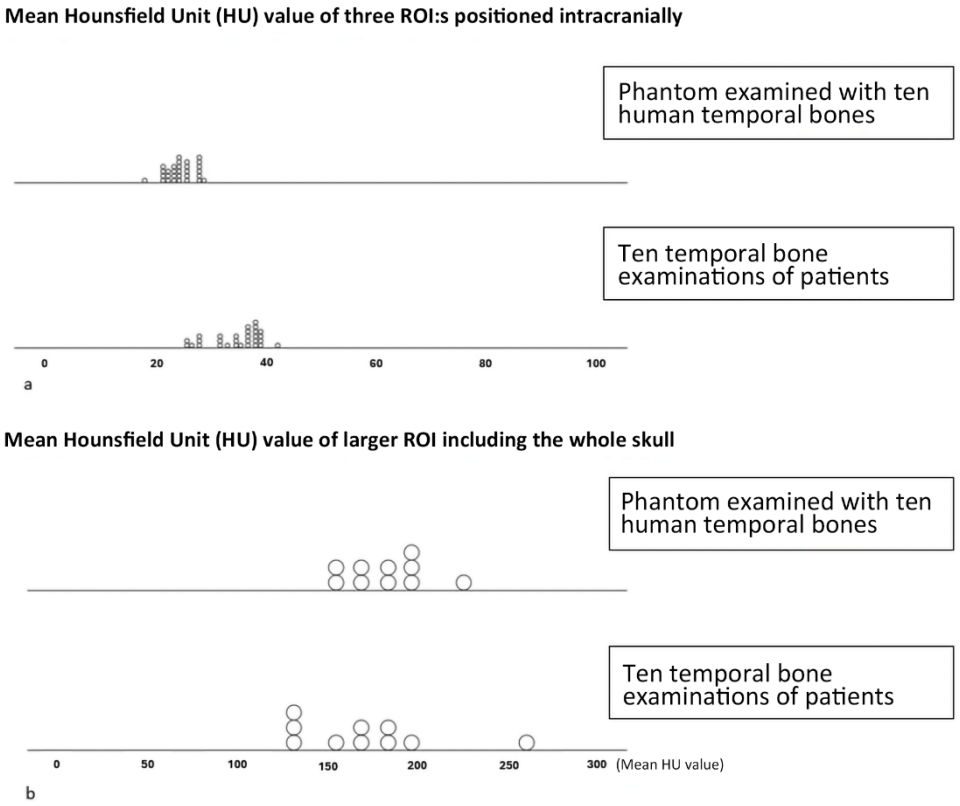

Figure 7 a) The mean Hounsfield unit value of three ROIs positioned intracranially (anthropomorphic skull phantom group = phantom examined with ten different human temporal bones; patient group = ten consecutive patients). b) The mean Hounsfield unit value of large ROI including the whole skull (anthropomorphic skull phantom group = phantom examined with ten different human temporal bones; patient group = ten consecutive patients).

The Mann-Whitney U test did not reveal a statistically significant difference in HU values between the two groups for the larger ROI containing the entire area of the head (Figure 7b).

3.2 Clinical Application

The phantom used for optimizing clinical protocols on different CBCT/CT scanners according to the methodology has been described in Figure 5. Detailed results, including technical parameters and dose values, have been presented in the additional files. These tests also revealed good reproducibility of the correct anatomical position of the temporal bone across different scanners (data not presented). Thus, the findings of this study suggest that the phantom is a reliable tool for facilitating the standardization and optimization of clinical protocols in radiological imaging.

4. Discussion

Information regarding the ground truth, which is difficult to obtain in clinical radiological trials [1], can be obtained using human temporal bone specimens that can be assessed and altered under a microscope. A modular anthropomorphic phantom with a specially designed chamber for the fixation of an exchangeable temporal bone was developed in this study. This facilitated the testing of different radiological settings in a reproducible manner, thereby enabling effective optimization of CT protocols for examining the middle ear. The phantom showed a good correlation with patients regarding attenuation and overall radiological assessability.

PUR plastic was selected owing to its similarities to soft tissues in radiological examinations, viscosity, and castability. The material's low viscosity aids in filling small cavities and ensures close contact between the dry skull and the plastic. In addition, PUR has a relatively short curing time but a sufficiently long shelf-life to be practical. Furthermore, PUR can be cast in several layers with good adhesion, which facilitates the initial fixation of the structures in the mold.

It would be advantageous to seal the sinus cavities to prevent the inflow of the PUR plastic; however, as the mean attenuation for actual patients is on par with the mean attenuation of the phantom (Figure 7b), this may result in no significant difference.

Alginate is used to make impressions in the field of dental reconstruction. Its characteristics proved to be better than those of ballistic gels for the fixation of temporal bones. The radiological attenuation of alginate is higher than that of soft tissue and brain tissue in this area; however, it was considered an equivalent for the tissues in this region, as it also replaced some of the bone missing from the temporal bone specimen and phantom dry skull.

An advantage of the phantom developed in this study over prefabricated phantoms is that it facilitates the swift exchange of bone specimens. Thus, different pathologies can be examined, enabling blinded radiological assessments and evaluations of inter-individual reliability.

The phantom can be used for several purposes, including optimizing protocols and training simulations to determine the consistency between experienced radiologists and identify spot rare injuries. It can also verify the degree of certainty with which specific injuries can be diagnosed using specific parameters.

Although several parameters had to be considered before selecting the final material for constructing the phantom and specimen jar, the proposed model fulfilled its purpose of producing a helpful phantom.

The potential harm should always be considered in clinical radiological settings. All radiological examinations must be justified and optimized, and the benefits to the patient must always exceed the potential risks. In many situations, conducting comparable prospective patient studies is unethical and expensive. The use of phantoms offers several advantages. Repetitive examinations can be performed using the same specimen for comparison when optimizing new protocols or evaluating new X-ray systems. The correct anatomy was obtained as the temporal bone specimen used was human. Moreover, aligning the temporal bone specimens in an anatomically correct position was easy.

The middle and inner ear structures are challenging to depict due to their minute size. Moreover, these structures are embedded in some of the densest bones in the body. The spatial resolution of high-contrast objects, such as the ossicles, was maximized when optimizing the protocol in the present study; thus, the highest tube current at a small focal spot was selected. Image quality is

strongly linked to the radiation dose, as noise in an image disturbs the ability to resolve objects. Low-contrast objects are affected by noise. Diagnosing temporal bone pathologies depends on the ability to image high-contrast objects (compact bone in relation to air and soft tissues). The size of the focal spot affects the details more than the radiation dose (i.e., noise) of high-contrast objects. Different-sized focal spots have limitations in terms of the tube current and potential; thus, the radiation dose is limited within each focal spot. Increasing the tube current (dose) above the maximum tube current for the focal spot in question resulted in the CT system automatically switching to a larger focal spot without informing the user.

The present study revealed that the phantom, emulating a living patient consists of a blend of PUR plastic, a dry human skull, and exchangeable freshly frozen human temporal bones. The average HU values of the larger ROIs did not exhibit any statistically significant differences between the patients and phantom.

Phantom is used in ongoing clinical diagnostic studies aiming to explore the advantages and limitations of different radiological modalities (CT, PCCT, and CBCT) for the detection of pathologies in the temporal bone, such as fractures of the ossicles, displacement of the middle ear prosthesis, and bony dehiscence.

5. Conclusion

The modular anthropomorphic phantom developed in this study can help optimize CT protocols for the middle ear and verifying diagnostic accuracy. Its ability to facilitate the swift exchange of bone specimens and reproduce examinations in a safe and controlled environment makes it a valuable tool in clinical practice and research. The modular phantom developed in this study can also be applied to other body parts. To our knowledge, no similar modular phantom has been reported in the literature or made available commercially.

Acknowledgments

We would like to thank the Radiology Department at Sunderby Hospital, Sweden, for allowing us to conduct our study on their machines. We would like to thank Robert Lundquist for valuable statistical support and Editage (www.editage.com) for English language editing. The study has been founded by the County Council of Norrbotten, Sweden and Umeå University, Sweden.

Author Contributions

All authors contributed to the study design. MVF and LK created the phantom. The sample jars for the fixation of the temporal bones and different fixation materials were evaluated and finalized using MVF, LK, and AR. Human temporal bones were fitted and fixed to a sample jar using AR. Tests on CT and CBCT were performed using MVF and LK and evaluated using MVF, LK, LF DB, and KT. All authors have read and contributed to the necessary changes and approved the final version of the manuscript.

Competing Interests

The authors declare that they have no conflict of interests.

References

1. Abadi E, Segars WP, Tsui BM, Kinahan PE, Bottenus N, Frangi AF, et al. Virtual clinical trials in medical imaging: A review. J Med Imaging. 2020; 7: 042805.
2. Samei E, Kinahan P, Nishikawa RM, Maidment A. Virtual clinical trials: Why and what (special section guest editorial). J Med Imaging. 2020; 7: 042801.
3. Goske MJ, Applegate KE, Boylan J, Butler PF, Callahan MJ, Coley BD, et al. The image gently campaign: Working together to change practice. Am J Roentgenol. 2008; 190: 273-274.
4. European Society of Radiology (ESR), European Federation of Radiographer Societies (EFRS). Patient safety in medical imaging: A joint paper of the European society of radiology (ESR) and the European federation of radiographer societies (EFRS). Radiography. 2019; 25: e26-e38.
5. Shrimpton PC, Wall BF, Fisher ES. The tissue-equivalence of the Alderson rando anthropomorphic phantom for x-rays of diagnostic qualities. Phys Med Biol. 1981; 26: 133.
6. Kashikar TS, Kerwin TF, Moberly AC, Wiet GJ. A review of simulation applications in temporal bone surgery. Laryngoscope Investig Otolaryngol. 2019; 4: 420-424.
7. Merken K, Monnens J, Marshall N, Johan N, Brasil DM, Santaella GM, et al. Development and validation of a 3D anthropomorphic phantom for dental CBCT imaging research. Med Phys. 2023; 50: 6714-6736.
8. Scarfe WC, Farman AG. What is cone-beam CT and how does it work? Dent Clin North Am. 2008; 52: 707-730.
9. Fahrig R, Jaffray DA, Sechopoulos I, Webster Stayman J. Flat-panel cone beam CT in the clinic: History and current state. J Med Imaging. 2021; 8: 052115.
10. Hermans R, Boomgaert L, Cockmartin L, Binst J, De Stefanis R, Bosmans H. Photon-counting CT allows better visualization of temporal bone structures in comparison with current generation multi-detector CT. Insights Imaging. 2023; 14: 112.
11. Pauwels R, Beinsberger J, Stamatakis H, Tsiklakis K, Walker A, Bosmans H, et al. Comparison of spatial and contrast resolution for cone-beam computed tomography scanners. Oral Surg Oral Med Oral Pathol Oral Radiol. 2012; 114: 127-135.
12. DenOtter TD, Schubert J. Hounsfield unit. Treasure Island, FL: StatPearls Publishing; 2024.
13. Horos Project. Homepage [Internet]. Horos Project; 2024. Available from: https://horosproject.org/.
14. Autodesk, Inc. Autodesk Meshmixer [Internet]. San Rafael, CA: Autodesk, Inc.; 2017. Available from: https://meshmixer.com/.
15. Dassault Systemes SolidWorks Corporation. Your place for all things SOLIDWORKS [Internet]. Waltham, MA: Dassault Systemes SolidWorks Corporation; 2018. Available from: https://my.solidworks.com/.
16. Nascimento EH, Fontenele RC, Lopes PD, Santaella GM, Vasconcelos KF, de Freitas DQ, et al. Development of a model of soft tissue simulation using ballistic gelatin for CBCT acquisitions related to dentomaxillofacial radiology research. Dentomaxillofac Radiol. 2021; 50: 20200191.